scientific reports

Check for updates

OPEN

Experimental study on disintegration of unsaturated red clay in Ca^{2+} solution environment

Hongming Wang[1,2], Zhikui Liu[1]✉, Shanmei Li[1] & Huajian Yang[1]

Guilin is a world-famous karst area characterized by a high concentration of Ca^{2+} in its groundwater. The disintegration of red clay plays a key role in the collapse of soil caves. In order to study the disintegration mechanisms of unsaturated red clay in Ca^{2+} solution, disintegration tests were conducted using a self-made disintegration apparatus. The soil samples are placed on the sieve plate of the disintegration apparatus, and a tensile meter records the real-time change of samples mass to calculate the disintegration rate. XRD analysis and filter paper method were employed to determine the mineral composition and matric suction of red clay, respectively. The results show that the matric suction decreases with increasing moisture content and increases with the void ratio. When the matric suction exceeds 965 kPa, disintegration is markedly intense, and the disintegration rate shows no significant correlation with Ca^{2+} concentration. When the matric suction is below than 965 kPa, the disintegration rate increases from 0.057 to 3.027 g/s with the increase of Ca^{2+} concentration. The disintegration of red clay with high matric suction is primarily attributed to the rapid ingress of water molecules and the compression of air due to matric suction, resulting in tensile stress. The disintegration of red clay with low matric suction is primarily caused by the reduction in the diffusion layer thickness of clay particles and the weakening of interparticle attraction due to Ca^{2+}.

Keywords Disintegration, Unsaturated red clay, Ca^{2+} solution, Diffusion layers, Moisture content

Guilin is a city with a temperate climate, characterized by an average annual temperature of 18.9 °C, a maximum temperature of 42 °C, and an annual average rainfall of 1949.5 mm. The warm and humid climate facilitates the leaching of groundwater, which dissolves limestone, calcite, and other minerals, thereby increasing the concentration of Ca^{2+} in the water. Red clay exhibits certain adsorption and chemical activity due to its rich minerals such as quartz, feldspar, free oxides, as well as clay minerals such as illite, montmorillonite, and kaolinite. Furthermore, the unique structural properties of red clay render it susceptible to disintegration upon exposure to water or chemical solutions, which can result in engineering geological hazards, such as soil caves collapse, roadbeds subsidence, landslides instability, and soil erosion[1–4]. The view that the disintegration of red clay is an important factor causing soil collapse is increasingly recognized[5–8]. However, existing literature mainly focuses on the decomposition of residual soil, expansive soil, loess, etc., with fewer studies addressing the disintegration of red clay. The current research is still not thorough enough. Therefore, this study aims to investigate the disintegration mechanisms of unsaturated red clay in the karst area of Guilin, focusing on the effects of elevated Ca^{2+} concentrations. The findings of this study will contribute to enhancing the ability to mitigate soil caves collapse.

Many studies have been conducted on the disintegration of soil and rock masses, revealing that factors such as mineral composition[9,10], physical state[11–13] (e.g., initial moisture content, liquid limit, plastic limit, saturation), soil structure characteristics[14–16] (e.g., porosity, void ratio, degree of compaction), environmental temperature[12,17,18], and the composition and concentration of aqueous solutions[19–21] significantly influence disintegration behavior. Tan[22] and Wang et al.[23] proposed that the chemical composition of water is a significant factor influencing the disintegration of red clay. Pang et al.[24] discovered that buildings located near sites where strong acid and alkaline industrial wastewater was discharged experience uneven settlement in their foundations, resulting in damage to the structures. They concluded that chemical solutions play a significant role in the disintegration of the red clay, ultimately leading to building damaged. Gupta et al.[25], Ghobadi et al.[26], Li et al.[27], respectively studied the effects of $(NH_4)_2CO_3$ solution, acid-base solution on the disintegration characteristics of shale, saturated red clay, and sandstone. Thyagaraj et al.[28], Mokni et al.[29], Zhang et al.[30], Wang et al.[31], found that the pore pressure

[1]College of Civil Engineering and Architecture, Guilin University of Technology, Guilin 541004, China. [2]Department of Construction Engineering, Guizhou Light Industry Technical College, Guiyang 550000, China. ✉email: 1998009@glut.edu.cn

Sample	Specific gravity	w_L liquid limit (%)	w_p plastic limit (%)	I_p plasticity index
The red clay	2.730	57	29	28

Table 1. Physical properties of Guilin red clay.

Sample	Relative clay mineral content (%)					
	Quartz (SiO_2)	Kaolinite	Illite	Mensuration stone	Iron oxide	Potassium feldspar
The red clay	44.8	18.4	27.3	–	5.8	3.7

Table 2. Main mineral composition of Guilin red clay.

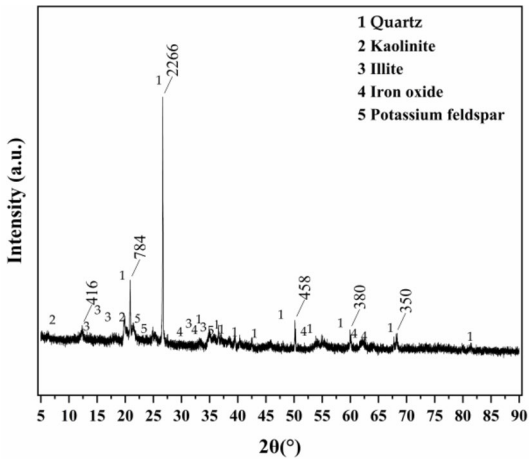

Fig. 1. XRD diffraction results. The mineral composition results of red clay tested by XRD.

and matrix suction in the soil are the main controlling factors for the disintegration of unsaturated soil. Fattah et al.[32], conducted disintegration tests on three types of gypseous soils using the oedometer deviceand found that the disintegration ability decreased as the matrix suction increased.

Numerous theories on the mechanism of rock and soil mass were proposed after conducting a large number of experiments. Caron et al.[33] considered that the main reason for the disintegration is the compression of enclosed gases in the soil by water molecules. Terzaghi[34], Cepeta[35] proposed the mechanism of 'gas-induced disintegration' is an important process in the disintegration of expansive rock. Tan et al.[36] suggested that the disintegration of mudstone is a water–rock (soil)–chemical coupling process of mineral expansion and salt dissolution. Pan et al.[37] used colloidal chemistry and fracture mechanics theory to establish a "water-rock" or "water-soil" interface model to describe the disintegration process from the perspective of hydration and diffusion of mineral particles.

Current research on the disintegration characteristics of red clay in karst region is still limited. The disintegration mechanism is primarily analyzed in terms of material composition and structural characteristics, while often neglecting the influence of the matrix suction of unsaturated red clay and the presence of Ca^{2+} in karst groundwater. This article aims to observe and record the disintegration processes of Guilin red clay with varying initial moisture content and void ratio in pure water and $CaCl_2$ solutions with concentrations of 0.05 mol/L, 0.1 mol/L, and 0.2 mol/L, using a self-made disintegration apparatus. The matrix suction of each soil sample was quickly determined using the filter paper method, and the disintegration mechanism of unsaturated red clay in pure water and Ca^{2+} solution are discussed comprehensively.

Analysis of red clay physical properties

The red clay used in the experiments was obtained from the foundation pit of the proposed teaching building at Guilin University of Technology (Yanshan Campus). The red clay was air-dried, purified, dried, and passed through a 0.5 mm standard sieve and tested for its liquid limit and plastic limit using a liquid plasticity limit combined apparatus, as shown in Table 1. The dried red clay was sieved through a 0.075 mm standard sieve and analyzed for its mineral composition using an X-ray diffractometer (XRD) instrument, as shown in Table 2; Fig. 1. The German Bruker D8 Advance X-ray powder diffraction instrument was used for XRD diffraction experiments. The testing conditions are as follows: Cu target [Ka radiation (0.15418 nm)], tube voltage of 40 kV, tube current of 25 mA, scanning speed of 10°/min, scanning angle from 5° to 90°.

Sample	Ca (ppb)	Na (ppb)	Mg (ppb)	Al (ppb)	K (ppb)	Fe (ppb)	Zn (ppb)
Groundwater	17958.0	1880.10	1305.55	33.69	864.54	24.23	0.857

Table 3. Main cation concentrations in Guilin groundwater.

Sample	Ca (ppb)	Na (ppb)	Mg (ppb)	Al (ppb)	K (ppb)	Fe (ppb)	Zn (ppb)
Pure water	62.33	18.22	6.3	7.83	0.75	1.62	Untested
The red clay + pure water	817.21	471.43	92.88	559.84	525.63	422.24	5.29

Table 4. Main cation concentrations in the supernatant after soaking red clay in pure water.

Figure 1 shows that quartz (SiO_2) exhibited the highest peak intensity and highest content in the XRD spectrum of Guilin red clay, making up 44.8% of the total mass. Its crystal lattice is stable, with a relatively small specific surface area and stable chemical properties. The main clay mineral components were Illites (27.3%) and Kaolinites (18.4%), with no Montmorillonite presented.

Illites are formed from silica-oxygen tetrahedrons and aluminum-hydroxide octahedra in a 2:1 ratio. The outer surfaces of illites expose the oxygen ions of the silica-oxygen tetrahedrons. Kaolinites are formed from silica-oxygen tetrahedrons and aluminum hydroxide octahedra in a ratio of 1:1. The outer surfaces of kaolinites expose the oxygen ions of the silicon-oxygen tetrahedrons and the hydroxyl ions of the aluminum-hydroxide octahedra. Therefore, clay minerals exhibit relatively active physicochemical properties.

There is a natural seasonal spring on the southwest side of the red clay collection site. The groundwater was taken and analyzed using the Agilent 7800 Inductively Coupled Plasma Mass Spectrometer(ICP–MS) purchased by our unit. ICP-MS tuning solution: a tuning solution containing Ce, Co, Li, Mg, Ti, and Y elements, with a concentration of 1 μg/L. The main cation concentrations of the natural groundwater is shown in Table 3. The concentration of Ca^{2+} in groundwater is much higher than that of other major cations. To verify that the soluble minerals in red clay dissolve in water, causing changes in the ions concentrations in groundwater, this paper separately tests the major ions concentrations in pure water and the supernatant of red clay + pure water, using the same testing method as for spring water. The method for preparing the supernatant after soaking red clay in water is as follows: The dried red clay was sieved through a 0.075 mm standard sieve. The 5 g of red clay was weighed using an electronic balance with a precision of 0.1 g. Then, it was mixed with pure water at a soil-to-water ratio of 1:5. After stirring with a glass rod for 5 min, it was allowed to stand for 30 min. The supernatant for testing was ready. The indoor temperature was kept constant at 20 °C with a humidity of 60% during the experiment. The test results are shown in Table 4. The results show that certain minerals in red clay dissolved in water, leading to an increase in the concentration of Ca^{2+} ions.

Unsaturated red clay disintegration test

Sample preparation and test equipment

Based on the geotechnical investigation reports, the natural moisture content of red clay in the Guilin area ranges from 24 to 31%, and the void ratio ranges from 0.98 to 1.15. Therefore, this paper selected two initial moisture contents of 24% and 28%, and three void ratios of 1.0, 1.1, and 1.15 to prepare six reshaping samples using an orthogonal design. The reshaped red clay sample is cylindrical, with a diameter of 60 mm, a height of 106 mm, and a volume of 300.0 cm^3. The method for making samples is as follows: The dried red clay was sieved through a 2 mm standard sieve, and a suitable amount of pure water was added to it, ensuring that its moisture content reaches 24% and 28% respectively, and then sealed and allowed to stand for 24 h. The masses of red clay required to make samples with different initial moisture content and void ratios were calculated according to formula (1), and then the red clay was weighed and divided into 4 equal parts and added to the mold sequentially. To ensure samples integrity, the surface of each layer of compacted soil was scarified to improve the connection between each layer of samples. The reshaped samples with a mass error within 0.5% were deemed suitable for subsequent disintegration tests[38,39]. The self-made disintegration apparatus is shown in Fig. 2.

$$m_s = G_s \frac{V}{1+e}(1 + 0.01\,\omega) \tag{1}$$

m_s represents the mass (g) of red clay required; G_s represents the specific gravity of red clay soil particles; V represents the volume (cm^3) of the red clay soil sample; w represents the initial moisture content (%) of red clay; e represents the void ratio of the red clay sample.

Once the preparation work was ready, the temperature controller probe was inserted into the center of the water tank to test the temperature of the disintegration solution first. If the temperature of the disintegration solution was below 20 °C, the temperature compensation device would be automatically started. If the temperature of the disintegration solution was too high, the dissolution solution would be naturally cooled to the set value, and the temperature deviation controlled within ± 0.5 °C. The tensile tester was zeroed after being started, and the soil sample was placed on the sieve plate. The change in soil sample mass was recorded every second with an accuracy of 1 g, while the disintegration process was observed.

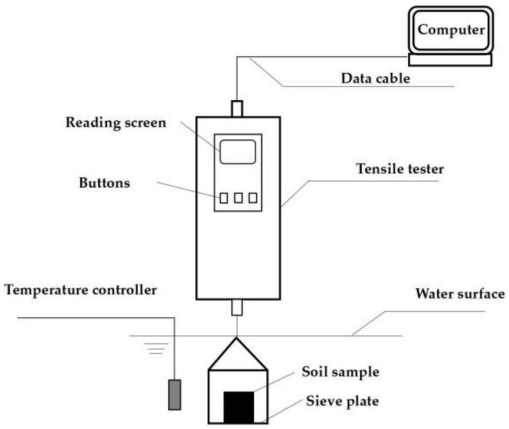

Fig. 2. Self-made disintegration apparatus. Installation diagram of self-made disintegration apparatus.

Disintegration solution	Pure water	$CaCl_2$ solution		
		0.05 mol/L	0.1 mol/L	0.2 mol/L
Experimental quantity (groups)	6	6	6	6

Table 5. Statistical table of disintegration test.

The disintegration rate and disintegration resistance index were calculated according to Formulae (2) and (3) respectively.

$$\upsilon = \frac{A_t^i - A_t^{i+1}}{t_{i+1} - t_i} \tag{2}$$

$$S_I = \frac{A_t^{max}}{A_0} \times 100\% \tag{3}$$

υ represents the disintegration rate (g/s) of the soil sample between ti and ti + 1; *Ai t* ,*Ai + 1 t* represent the mass (g) of the soil sample at time ti and ti + 1, respectively; t_i, t_{i+1} represent the time (s) during the experiment; S_I represents the disintegration resistance index (%); A_0, *Amax t* represent the mass of the soil sample at the beginning and end of the disintegration process, respectively (g).

Experimental design

In order to study the disintegration characteristics of unsaturated red clay in pure water and Ca^{2+} solutions, each unsaturated red clay was placed in pure water and $CaCl_2$ solutions with concentrations of 0.05 mol/L, 0.1 mol/L, and 0.2 mol/L respectively. The solute $CaCl_2$ for the experiment was from China National Pharmaceutical Group Chemical Reagent Co., Ltd., with a purity of 99.5%. The solvent was pure water, the pure water used in the experiments was prepared by the YAZD-5 type electrothermal purified water sterilizer in the on-campus laboratory. The quality of pure water meets the third-level water standard specified by the People's Republic of China. The conductivity of purified water is ≤ 0.50 mS/m, the content of oxidizable substances is ≤ 0.4 mg/L, and the residue after evaporation is ≤ 2.0 mg/L. The experimental plan is shown in Table 5.

Disintegration characteristics of unsaturated red clay

Disintegration characteristics of unsaturated red clay in pure water

The 24% of red clay samples disintegrate more violently in pure water. The 24% red clay with e = 1.0 disintegrate relatively quickly, and the soil particles rapidly disintegrate into scales and fragments. The mass of the soil remains basically unchange after 450 s. The disintegration rate is 0.739 g/s, and the disintegration resistance index is 38.42%. When e = 1.1 and 1.15, the soil sample undergo explosive and intense disintegration. The disintegration solution become turbid, and a large number of bubbles escape, causing the disintegration rate to increase sharply. The soil completely disintegrate, with disintegration rates of 1.769 g/s and 2.813 g/s respectively, which are 139.3% and 59.0% higher than the previous void ratio. The disintegration rate of red clay with a moisture content of 24% increase significantly with an increase in void ratio. Additionally, the resistance to disintegration index decrease dramatically, indicating a more intense disintegration phenomena.

The 28% of red clay samples disintegrate very slowly or do not disintegrate in pure water. When e = 1.0, there is still no debris falling after the soil sample is soaked for 2000 s, and the mass of the soil sample increase by 8 g, indicating that the soil's moisture content increase due to matrix suction after encountering water. When e = 1.1 and e = 1.15, the red clay disintegrate slowly, and the soil disintegrate into fragments. The pure water is relatively

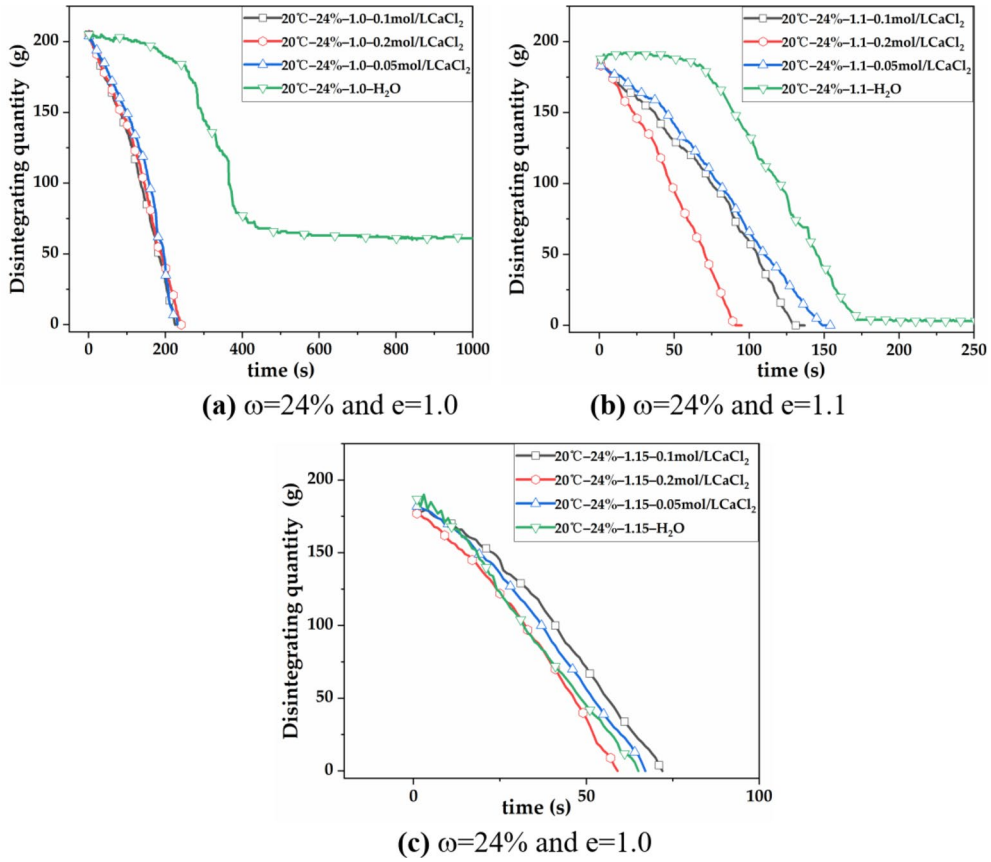

Fig. 3. Disintegration curves of red clay with w = 24% in pure water and $CaCl_2$ solution. (**a**) Disintegration curves of red clay with w = 24%, e = 1.0 in each solution; (**b**) Disintegration curves of red clay with w = 24%, e = 1.1 in each solution; (**c**) Disintegration curves of red clay with w = 24% and e = 1.15 in each solution.

Moisture content (%)	Void ratio	The disintegration rate (g/s)			
		Pure water	0.05 mol/L $CaCl_2$	0.1 mol/L $CaCl_2$	0.2 mol/L $CaCl_2$
24	1.0	0.739	0.886	0.915	0.961
	1.1	1.769	1.23	1.442	2.1
	1.15	2.813	2.727	2.507	3.052
28	1.0	0	0.057	0.148	0.2
	1.1	0.029	0.088	0.212	0.232
	1.15	0.036	1.361	3.016	3.063

Table 6. The disintegration rate of unsaturated red clay.

clear, and no bubble overflow is observed. The disintegration rates are 0.029 g/s and 0.036 g/s respectively, with disintegration resistance indices of 98.1% and 85.8%. The disintegration rate of red clay with ω = 28% increase slightly with the increase of void ratio, and the disintegration resistance index decrease significantly. The disintegration phenomena are all very gentle.

When e = 1.0, the 28% of red clay do not undergo significant disintegration, and the disintegration rate is 0.739 g/s lower than that of the red clay with w = 24%. When e = 1.1 and e = 1.15, the disintegration rates decrease by 1.74 g/s and 2.777 g/s respectively, with reduction rates of 98.3% and 98.7% respectively. The disintegration phenomenon also gradually become gentle. When the void ratio remains constant, the disintegration rate gradually decreases with increasing moisture content. Additionally, the disintegration resistance index significantly increases.

Disintegration characteristics of unsaturated red clay in Ca2+ solution

Figure 3; Table 6 show the disintegration rate of red clay with w = 24% and e = 1.0 in 0.05 mol/L $CaCl_2$ solution is 0.886 g/s. The soil particles rapidly disintegrate into fragments and mud, with a slight increase in disintegration rate of 0.147 g/s compared to pure water, representing a 19.9% increase. The disintegration resistance index drops

from 38.42% to 0. When the solution concentration is 0.1 mol/L, the soil sample completely disintegrates, the disintegration phenomenon is more intense, the complete disintegration time is shorter, and the disintegration rate is 0.915 g/s, an increase of 3.2%. When the solution concentration is 0.2 mol/L, the soil completely disintegrates within 240 s and the phenomenon is the most intense, with a maximum disintegration rate of 0.961 g/s, an increase of 5.0%.

It can be seen that the disintegration rate of red clay with w = 24% and e = 1.0 in $CaCl_2$ solutions at various concentrations is higher than that in pure water, and it increases with the concentration of Ca^{2+}. The disintegration rates of red clay with moisture content of 24%, e = 1.1 and e = 1.15 in various concentrations of $CaCl_2$ solution fluctuate slightly with the increase of Ca^{2+} concentration, and the disintegration phenomenon is very intense. This may be because the red clay with low moisture content has a large matrix suction, and Ca^{2+} enters the pores before fully participating in the physical and chemical reactions of the soil sample, leading to disintegration. Therefore, the influence of Ca^{2+} on the disintegration characteristics of red clay with low moisture content and high void ratio is not significant, and the disintegration mechanism cannot be revealed using the double layer theory. When the Ca^{2+} concentration is constant, the disintegration rate of red clay with w = 24% increases as the void ratio increases.

According to Fig. 4; Table 6, the red clay with w = 28% and e = 1.0 slowly disintegrates in a 0.05 mol/L $CaCl_2$ solution, with a disintegration rate of 0.057 g/s and a disintegration resistance index of 66.7%, the degree of disintegration is significantly increased compared to that in pure water. When the Ca^{2+} concentration is 0.1 mol/L, the disintegration rate reaches 0.148 g/s, with an increase of 159.6% and a disintegration resistance index of 64.8%. When the Ca^{2+} concentration is 0.2 mol/L, the disintegration rate is 0.2 g/s, with an increase of 35.1%. The soil has completely disintegrated. The red clay with w = 28% and e = 1.1 disintegrates rapidly in a 0.05 mol/L $CaCl_2$ solution. The disintegration rate is 0.088 g/s and the disintegration resistance index is 76.5%, indicating a significant increase in disintegration degree. When the Ca^{2+} concentration is increased to 0.1 mol/L, the disintegration rate reaches 0.212 g/s, which is a 140.9% increase, and the soil completely disintegrates. When the Ca^{2+} concentration is 0.2 mol/L, the disintegration rate is 0.232 g/s, with an increase of 9.4%, and the soil completely disintegrates. The red clay with w = 28% and e = 1.15 disintegrates very quickly in a 0.05 mol/L $CaCl_2$ solution, with a disintegration rate of 1.325 g/s higher than that in pure water, reaching 1.361 g/s, and the soil completely disintegrates. The 28% red clay samples with e = 1.15 disintegrate completely in 0.1 mol/L and 0.2 mol/L $CaCl_2$ solutions, with disintegration rates of 3.016 g/s and 3.063 g/s, respectively, representing an increase of 121.6% and 1.5%.

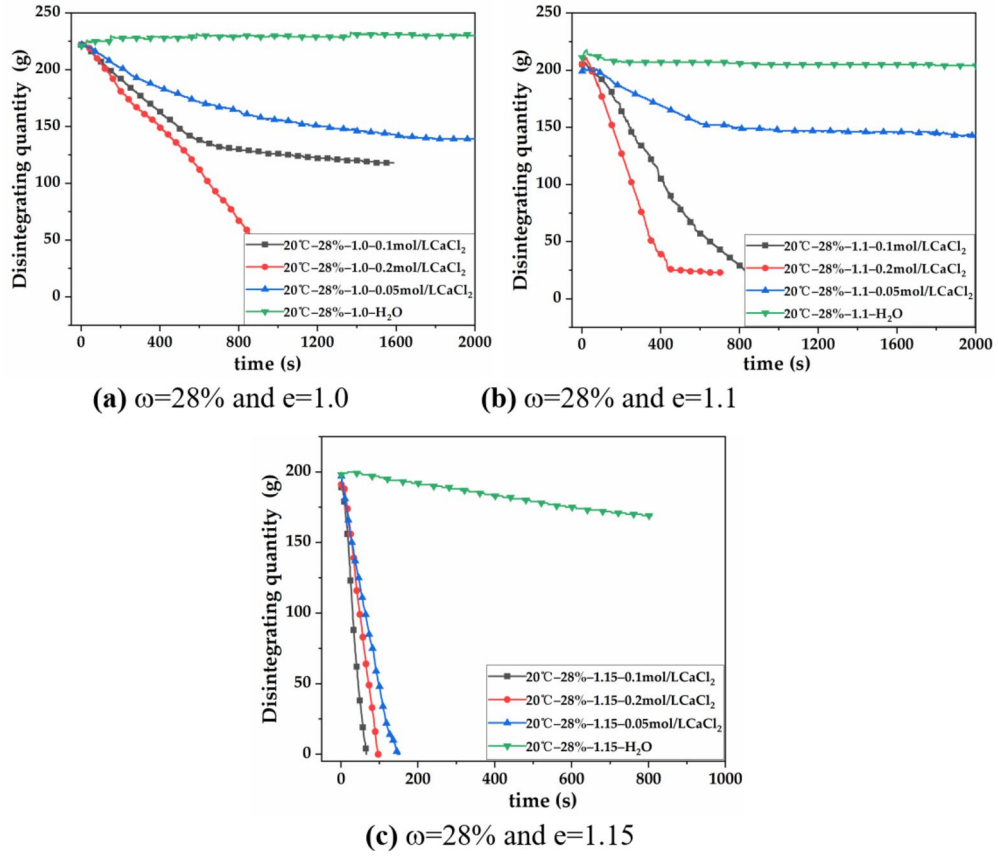

Fig. 4. Disintegration curves of red clay with w = 28% in pure water and Ca^{2+} solution. (**a**) Disintegration curves of red clay with w = 28%, e = 1.0 in each solution; (**b**) disintegration curves of red clay with w = 28%, e = 1.1 in each solutions; (**c**) disintegration curves of red clay with w = 28%, e = 1.15 in each solution.

Moisture content (%)	Void ratio	Disintegration rate in pure water (g/s)	Moisture content of intermediate layer filter paper (%)	Matrix suction (kPa)
24	1.0	0.739	29.13	965
	1.1	1.769	24.00	1585
	1.15	2.813	23.35	1810
28	1.0	0	37.67	256
	1.1	0.029	34.60	413
	1.15	0.036	32.37	584

Table 7. Matric suction of red clay at 20℃ (according to filter paper method).

Red clay categories	Fitting equations	Adjusted R^2	Fitting effect
High matrix suction	$\upsilon = 0.0023 \times s + 1.547$	0.86	good
Low matrix suction	$\upsilon = 0.0011 \times s - 0.0237$	0.746	general

Table 8. Fitting equations between disintegration rate and matrix suction.

It is evident that the disintegration rate of red clays with w = 28% is higher in $CaCl_2$ solutions of different concentrations than in pure water, and the disintegration resistance index gradually decreases. Ca^{2+} has a significant promoting effect on the disintegration of red clay. When the void ratio remains constant, the disintegration rate of the 28% red clay increases with the increase of Ca^{2+} concentration. However, the disintegration rate increase gradually decreases and the disintegration resistance index also gradually decreases. When the Ca^{2+} concentration is constant, the disintegration rate of the 28% red clay increases with the increase of void ratio, and the disintegration resistance index gradually decreases.

Relationship between the disintegration rate and the matrix suction

The filter paper method was employed to measure the matric suction of different unsaturated red clays, with the aim of investigating the relationship between the disintegration rate and the matric suction. The filter paper method, which measures matric suction (or total suction), is advantageous due to its simple principle, low cost, high accuracy, and wide measuring range.

This article used the filter paper method (ASTM D5298-10) recommended by the American Society of Testing Materials to test the matrix suction. The experimental method is briefly described as follows: Three filter papers were overlaid and placed flat between two circular soil samples with the same void ratio and initial moisture content. The diameter of the soil sample was 61.8 mm and the height was 20 mm. Subsequently, the two soil samples were fixed together with insulating tape to ensure tight contact between the soil sample and the filter paper. The samples were then placed in a sealed container and kept in a constant temperature environment at 20 °C. The three layers of filter paper were taken out 15 days later, and the uncontaminated middle layer of filter paper was placed on an electronic balance with an accuracy of 0.1 mg for rapid measurement of the paper's mass and calculation of the paper's moisture content. Finally, the matric suction of the soil sample was determined based on the calibration equation of the filter paper.

The calibration equation of Whatman No. 42 filter paper uses the bilinear calibration curve equation given by Leong et al.[40] to calculate the matric suction of each samples. The results are shown in the Formulae (4):

$$\begin{cases} lgs = 2.909 - 0.0229\omega_f;\ \omega_f \geq 47 \\ lgs = 4.945 - 0.0673\omega_f;\ 26 \leq \omega_f < 47 \\ lgs = 5.310 - 0.0879\omega_f;\ \omega_f < 26 \end{cases} \quad (4)$$

s represents matric suction (kPa); w_f represents the moisture content of the filter paper (%).

To explore the relationship between matric suction and the disintegration rate, while excluding the influence of Ca^{2+} on the disintegration rate of red clay, only the disintegration rate of each group of red clay in pure water was selected. The matric suction and disintegration rate for each unsaturated red clay are shown in Table 7.

Table 7 shows that the matric suction of red clay with the same moisture content increases as the void ratio increases, while the matric suction of red clay with the same void ratio decreases as the moisture content increases. The disintegration rate of each group of red clay increases with the matric suction. When the matric suction exceeds 965 kPa, the disintegration rate of red clay ranges from 1.769 to 2.813 g/s, the disintegration phenomena are also very intense. The disintegration rate shows no significant change with increasing Ca^{2+} concentration. When the matric suction is less than 965 kPa, the disintegration phenomena of red clay are relatively gentle, and the disintegration rate ranges from 0 to 0.739 g/s. The disintegration rate of each soil sample increases with the Ca^{2+} concentration. Therefore, based on the matric suction, unsaturated red clay can be divided into two categories to discuss the relationship between disintegration rate and matric suction. The fitting equation between the disintegration rate and matrix suction as shown in Table 8.

Disintegration mechanism of unsaturated red clay in Ca2+ solution

The Guilin red clay contains small clay mineral particles with a large specific surface area. The clay minerals have multiple static electric fields due to isomorphous substitution and exposed siloxane and alumina chemical groups on the surface. Moreover, the underground water in karst areas contains Ca^{2+}, which results in a double electric layer structure on the surface of clay minerals. When the composition of pore solution changes, it affects the thickness of the double layer, which in turn alters the interparticle interaction forces. This can cause the red clay to exhibit varying engineering characteristics[41]. Based on the disintegration tests of various red clays, It was found that the disintegration mechanisms of red clays with different matric suction were not consistent in pure water and Ca^{2+} solution environments, which can be summarized as follows:

The unsaturated red clay with high matrix suction encounters water, causing water molecules or chemical solutions to rapidly enter the soil under the strong matrix suction, compressing the enclosed gas sharply, and the additional tensile stress in the pores increases instantaneously. Ca^{2+} does not fully participate in physical and chemical changes, causing the red clay to disintegrate and a large amount of gas to escape. Therefore, matric suction is the main driving force for the disintegration of unsaturated red clay with high matrix suction, Ca^{2+} does not have a significant promoting effect on the disintegration of red clay.

The unsaturated red clay with low matrix suction encounters water, causing water molecules firstly enter the diffusion layer under the action of matrix suction and osmotic pressure, the thickness of the diffusion layer increases, the distance between two clay particles increases, and the short-range attraction decreases significantly. Once the short-range attraction cannot resist the thermal kinetic energy of the particles, the soil will irreversibly disintegrate. In addition, there is a "wedge cracking" tension between adjacent clay particles, which is also an important factor leading to disintegration, as shown in Fig. 5.

The unsaturated red clay with low matrix suction encounters Ca^{2+} solution, Ca^{2+} gradually enters the soil under the action of osmotic pressure and matrix suction. Ca^{2+} enter the diffusion layer firstly, increasing the concentration of Ca^{2+}, and the diffusion layer becomes thinner, the interparticle short-range attraction gradually decreases, leading to the disintegration of the red clay, as shown in Fig. 6. The higher the concentration of Ca^{2+}, the greater the osmotic pressure, the faster the Ca^{2+} enters the soil, the more severe the shrinkage of the diffusion layer, the more the interparticle attractive force between clay particles decays, and the rate of disintegration also increases with the increase of Ca^{2+} concentration. Therefore, Ca^{2+} plays a crucial role affecting the thickness of the clay double layers and the disintegration phenomena of red clay with low matrix suction.

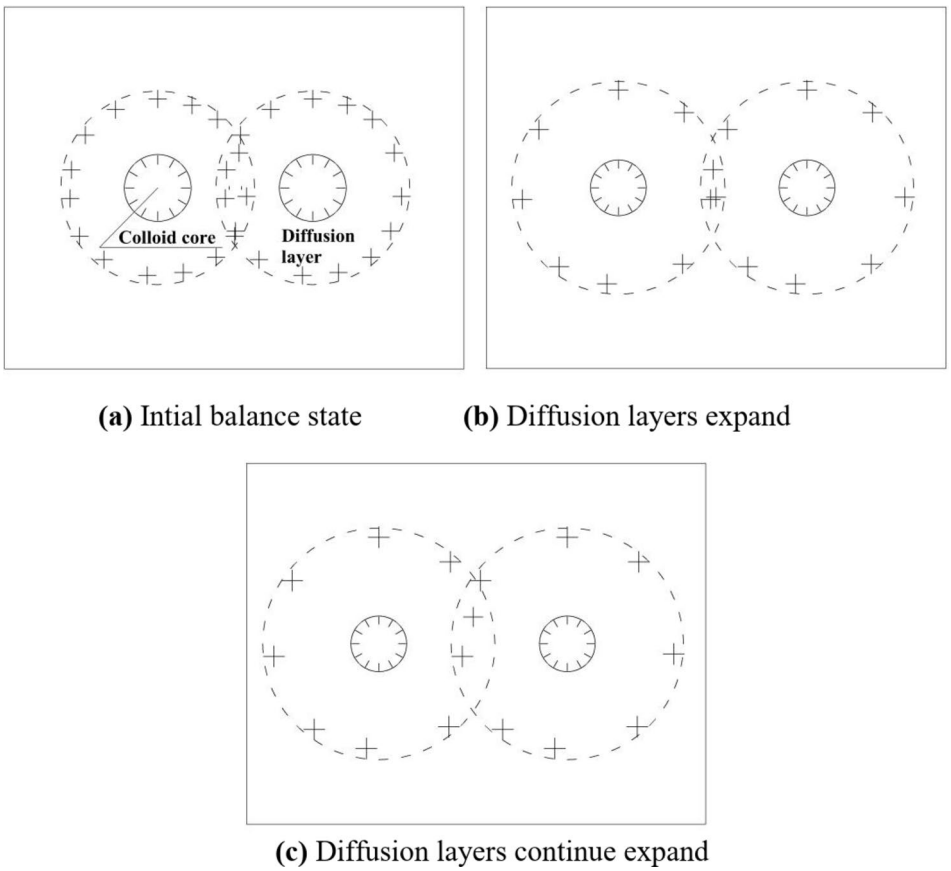

Fig. 5. The clay particle diffusion layers change during the disintegration in pure water. Schematic diagram of the changes in the clay particle diffusion layers during the disintegration of low matrix suction red clay in pure water. (**a**) Initial balance state. (**b**) Diffusion layers expand. (**c**) Diffusion layers continue expand.

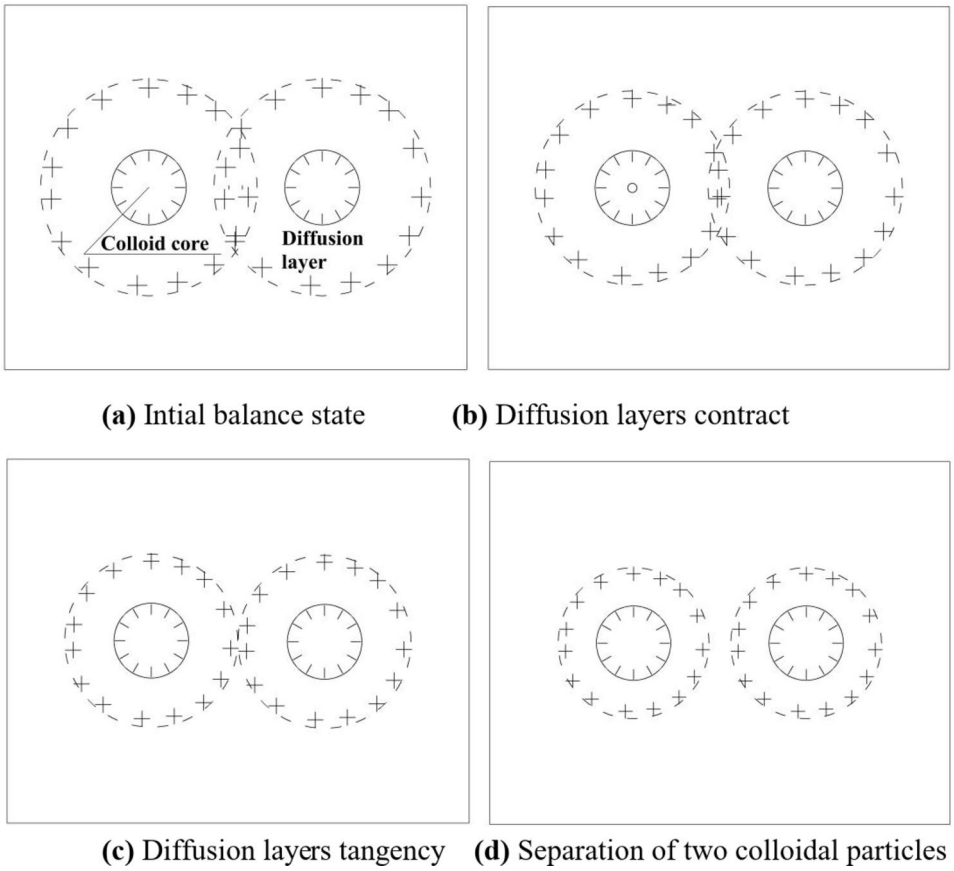

Fig. 6. The clay particle diffusion layers change during the disintegration in Ca^{2+} solution. Schematic diagram of the changes in the clay particle diffusion layers during the disintegration of low matrix suction red clay in $CaCl_2$ solution.

Conclusions

In this study, the mineral composition of Guilin red clay and the concentration of major cations in groundwater in karst areas were analyzed using X-ray diffractometer (XRD) instrument and Inductively Coupled Plasma Mass Spectrometer(ICP–MS) respectively. The matrix suction of each red clay sample was determined using the filter paper method. Subsequently, disintegration experiments of red clay with different matrix suction were conducted in pure water and three concentrations of $CaCl_2$ solution. The disintegration characteristics of red clay were found to be related to its matrix suction and there exists a threshold. The red clay was divided into two categories based on matrix suction threshold: high matrix suction red clay and low matrix suction red clay. The disintegration mechanisms of each category was discussed separately. The main conclusions are as follows:

1. The Guilin red clay contains abundant clay minerals such as kaolinite and illite, as well as free oxides. The groundwater in Guilin City contains a large amount of Ca^{2+} ions, and its concentration far exceeds that of other cations.
2. For unsaturated red clay, the moisture content remains constant, and the matrix suction increases with the increase of void ratio. the void ratio is constant, the matrix suction decreases with the increase of moisture content.
3. The disintegration rate of unsaturated red clay increases with an increasing void ratio at a constant moisture content. Conversely, when the void ratio remains constant, the disintegration rate decreases as moisture content increases. The disintegration rates of all red clays increase with an increasing matrix suction. When the matric suction exceeds 965 kPa, the red clay experiences rapid disintegration, with the disintegration rate ranging from 1.769 to 2.813 g/s. Conversely, when the matric suction is below 965 kPa, the disintegration rate is slower, ranging from 0 to 0.739 g/s. Therefore, the red clay is divided into two groups: high matrix suction red clay and low matrix suction red clay, with 965 kPa as the matrix suction threshold.
4. The unsaturated red clay with high matrix suction disintegrates more severely in pure water, and the disintegration rate is related to the matrix suction with a relationship $\upsilon = 0.0023 \times s - 1.547$, and the adjusted R^2 is 0.860. The greater the matrix suction, the greater the disintegration rate. The main disintegration mechanism is that the matric suction allows pure water to rapidly enter the soil, compressing and sealing the air, and the additional tensile stress generated leads to disintegrate. The effect of Ca^{2+} on the disintegration rate is not significant.

5. The unsaturated red clay with low matrix suction disintegrates more slowly in pure water, and the disintegration rate is related to the matrix suction with a relationship $\upsilon = 0.0011 \times s - 0.0237$,and the adjusted R^2 is 0.746. The main disintegration mechanism is that water molecules enter the soil under the action of osmotic pressure and matrix suction. The ion concentration in the diffusion layer is diluted, the diffusion layer slowly thickens, and the attraction between adjacent clay particles weakens, resulting in soil disintegration.
6. Ca^{2+} significantly promotes the disintegration of unsaturated red clay with low matrix suction. The disintegration rate of w = 28%, e = 1.0, 1.1, and 1.15 in 0.05 mol/L $CaCl_2$ solution increased by 0.057 g/s, 0.059 g/s, and 1.325 g/s respectively compared to pure water. When $CaCl_2$ is 0.1 mol/L, the disintegration rate of ω = 28%, e = 1.0, 1.1, and 1.15 increased by 0.091 g/s, 0.124 g/s, and 1.655 g/s respectively. When $CaCl_2$ is 0.2 mol/L, the disintegration rate increased by 0.052 g/s, 0.02 g/s, and 0.047 g/s respectively. In other words, the disintegration rate of low matrix suction red clay increases as the Ca^{2+} concentration increases, but the rate of increase decreases. The primary disintegration mechanism is that Ca^{2+} reduces the thickness of the clay particle diffusion layer. The resulting increase in particle spacing and decrease in particle attraction are the fundamental causes of disintegration.

Data availability

All data generated or analysed during this study are included in this published article.

Received: 24 April 2024; Accepted: 27 November 2024
Published online: 03 December 2024

References

1. Alavi Nezhad, S. V., Abad, K., Tugrul, A., Gokceoglu, C. & Jahed, D. Characteristics of weathering zones of granitic rocks in Malaysia for geotechnical engineering design. *Eng. Geol.* **200**, 94–103 (2016).
2. Pradhan, A. & Kim, Y. T. Application and comparison of shallow landslide susceptibility models in weathered granite soil under extreme rainfall events. *Environ. Earth Sci.* **73**, 5761–5771 (2015).
3. Qi, Y., Jiang, P. & Liu, X. Influence of soil disintegration in water on slope stability. *Chin. J. Geotech. Eng.* **42**(S2), 214–218 (2020).
4. Qiu, Z., Yang, Y. & Wu, Y. Experimental study on the disintegration characteristics of weakly weathered mudstone. *Sci. Technol. Eng.* **14**(12), 266–269 (2014).
5. Huang, F., Zhao, L., Ling, T. & Yang, X. Rock mass collapse mechanism of concealed karst cave beneath deep tunnel. *Int. J. Rock. Mech. Min. Sci.* **2017**, 133–138 (2017).
6. He, K., Jia, Y., Chen, W., Wang, R. & Luo H. Evaluation of karst collapse risks induced by over-pumping and karst groundwater resource protection in Zao-zhuang region, China. *Environ. Earth* **2014**, 3443–3454 (2014).
7. Haji, K. & Kamal, T. Hazards and mechanism of sinkholes on Kabudar Ahang and Famenin plains of Hamadan, Iran. *Nat. Hazards* **55**, 481–499 (2010).
8. Klimchouk, A. & Andrejchuk, V. Karst breakdown mechanisms from observations in the gypsum caves of the Western Ukraine: implications for subsidence hazard assessment. *Environ. Geol.* **48**, 336–359 (2005).
9. Jiang, F., Li, L. & Chen, H. Study on the critical conditions of karst collapse development in Guiyang Yongwen Middle School. *Chin. J. Karst* **37**(02), 294–299 (2018).
10. Liu, C. & Lu, S. Study on the softening mechanism of mudstone disintegration by water. *Rock Soil Mech.* **1**, 28–31 (2000).
11. Ruiz-Vera, V. & Wu, L. Influence of sodicity clay mineralogy, prewetting rate and their interaction on aggregate stability. *Soil Sci. Soc. Am. J.* **70**, 1825–1833 (2006).
12. Liu, B., Wang, L., Zhou, H. & Yang, B. Xiao, W. Experimental study on disintegration of Guilin. *Red Clay Sustain.* **15**, 7833. https://doi.org/10.3390/su15107833 (2023).
13. Zhou, C., Jing, X. & Liu, Z. Study on the characteristics and modification of weathered soil collapse in South China red bed. *J. Eng. Geol.* **27**(06), 1253–1261. https://doi.org/10.13544/j.cnki.jeg.2018-288 (2019).
14. Li, J., Cui, S. & Tian, W. Characteristics of rainfall erosion and soil disintegration experiment on highway slopes. *J. Chang'an Univ.* **1**, 23–26 (2007).
15. Tong, D., Feng, D. & Huang, S. Experimental study on the collapse characteristics of compacted soil. *Sci. Technol. Eng.* **18**(15), 129–136 (2018).
16. Tang, J., Yu, P., Wei, H. & Meng, Q. Experimental study on the disintegration characteristics of residual soil on Guizhou basalt. *J. Eng. Geol.* **19**(05), 778–783 (2011).
17. Zhang, D., Chen, A. & Su, Y. Influence of hydrothermal environment on the weathering characteristics of different purple mother rocks. *Acta Pedol. Sin.* **50**(04), 643–651 (2013).
18. Zeng, Q., Liu, B. & Zhang, B. Experimental study on the disintegration characteristics of red clay. *Hydrogeol. Eng. Geol.* **45**(03), 93–97. https://doi.org/10.16030/j.cnki.issn.1000-3665.2018.03.12 (2018).
19. Sun, B., Cai, H. & Zhang, Q. Experimental and discrete element simulation study on disintegration of marine weathered granite. *J. Xuzhou Univ.* **38**(04), 58–67. https://doi.org/10.15873/j.cnki.jxt.000534 (2023).
20. Ruan, Y., Liu, G. & Liu, Z. Influence of acid environment on disintegration characteristics of red mudstone highway subgrade filler. *Saf. Environ. Eng.* **28**(05), 75–79. https://doi.org/10.13578/j.cnki.issn.1671-1556.20201064 (2021).
21. Zuo, Q., Wu, L., Luo, T., Bian, Y. & Tan, Y. Study on macroscopic failure characteristics and microscopic mechanism of Yaogu tunnel in Shanghai–Kunming high-speed railway. *Hydrogeol. Eng. Geol.* **42**(01), 65–69 (2015).
22. Tan, J. Study on the mechanism of soil layer collapse in karst areas with full coverage in Guangxi. *J. Eng. Geol.* **9**(3), 272–276 (2001).
23. Wang, Z., Gao, W. & Liu, F. Analysis of soil disintegration and influencing factors in ground collapse area of Guilin Karst. *Geotech. Fund.* **31**(01), 59–62 (2017).
24. Pang, C., Lai, L. & Zhou, M. Chemical activity and engineering environmental effects of red clay in Guilin City. *Mineral. Resour. Geol.* **6**, 357–359 (2002).
25. Gupta, V. & Ahmed, I. The effect of pH of water and mineralogical properties on the slake durability (degradability) of different rocks from the Lesser Himalaya, India. *Eng. Geol.* **95**(3–4), 79–87 (2007).
26. Ghobadi, M. & Mousavi, S. The effect of pH and salty solutions on durability of sandstones of the Aghajari formation in Khouzestan province, southwest of Iran. *Arab. J. Geosci.* **7**(2), 641–653 (2014).
27. Li, S., Liu, Z. & Meng, J. Disintegration effect of saturated red clay under the action of $(NH_4)_2CO_3$. *J. Yangtze River Sci. Res. Inst.* **38**(11), 115–120 (2021).
28. Thyagaraj, T. & Das, A. P. Physico-chemical effects on collapse behaviour of compacted red soil. *Geotechnique* **67**, 559–571 (2017).
29. Mokni, N., Romero, E. & Olivella, S. Chemo-hydro-mechanical behaviour of compacted Boom Clay: Joint effects of osmotic and matric suctions. *Géotechnique* **64**, 681–693 (2014).

30. Zhang, S. Tang, H. Experimental study on weathering mechanism of unsaturated granite residual soil. *Rock Soil Mech.* **34**, 1668–1674 (2013).
31. Wang, J., Xiang, W. & Bi, R. Experimental study on the influence of matric suction on the disintegration of unsaturated remolded loess. *Rock Soil Mech.* **32**(11), 3258–3262 (2011).
32. Fattah, M. Y. & Dawood, B. A. Time-dependent collapse potential of unsaturated collapsible gypseous soils. *World J. Eng.* **17**, 283–294. https://doi.org/10.1108/WJE-09-2019-0276 (2020).
33. Caron, J., Espindola, C. & Angers, D. Soil structural stability during rapid wetting: influence of land use on some aggregate properties. *Soil Sci. Soc. Am.* **60**(3), 901–908 (1996).
34. Terzaghi, K. *Theoretical Soil Mechanics* (Wiley, 1943).
35. Cepeda, A. *An Experimental Investigation of the Engineering Behavior of Natural Shales*. Ph.D. Thesis, University of Illinois, Urbana-Champaign, Champaign, IL, USA (1987).
36. Tan, X. *Study on the Disintegration Characteristics of Mudstone Under the Action of Hydraulic-Chemical Erosion*. MA. Thesis, Liaoning Technical University, Liaoning, China (2016).
37. Pan, Y., Liu, Z. & Zhou, C. Experimental study on water-induced disintegration characteristics of red layer soft rock and its interface model. *Rock Soil Mech.* **38**(11), 3231–3239 (2017).
38. Wang, H., Liu, Z., Xie, Y. & Li, S. Experimental study on the disintegration behavior of red clay under different pH conditions. *Front. Mater.* **11**, 1477269 (2024).
39. Wang, H., Liu, Z., Xie, Y. & Li, Y. Study on the influence of moisture content and void ratio on the disintegration of red clay. *Appl. Sci.* **14**(9), 3652 (2024).
40. Leong, E., He, L. & Rahardjo, H. Factors affecting the filter paper method for total and matric suction measurements. *Geotech. Test. J.* **25**(3), 322–332 (2002).
41. Tang, D. & Sun, S. *Geotechnical Engineering* 2nd edn (Geological Publishing House, 2005).

Acknowledgements

The majority of the work presented in this paper was funded by National Natural Science Foundation of China (Grant No.41867039 and Grant No.52268055), the Guangxi Key Laboratory of Geomechanics and Geotechnical Engineering (No. 20-Y-XT-03), Fou-ndation Engineering of Technical Innovation Center of Mine Geological Environmental in Southern Area (No. CXZX2020002), the Guangxi Science and Technology Program (No.2022JJB160082).

Author contributions

The authors confirm contribution to the paper as follows: study conception and design: Wang Hongming, Liu Zhikui; data collection: Wang Hongming, Li Shanmei; analysis and interpretation of results: Wang Hongming, Yang Huajian, Li Shanmei; draft manuscript preparation: Wang Hongming, Liu Zhikui, Li Shanmei, Yang Huajian; All authors reviewed the results and approved the final version of the manuscript.

Declarations

Competing interests

The authors declare no competing interests.

Additional information

Correspondence and requests for materials should be addressed to Z.L.